Title:	**Structural Design Considerations and Challenges for Busan's Haeundae Resort Complex**
Author:	Kwang Ryang Chung, President, Dong Yang Structural Engineers
Subjects:	Building Case Study Structural Engineering
Keywords:	Belt Wall Concrete Construction Fire Safety Foundation Performance Based Design Residential Supertall
Publication Date:	2016
Original Publication:	Cities to Megacities: Shaping Dense Vertical Urbanism
Paper Type:	1. Book chapter/Part chapter 2. Journal paper 3. **Conference proceeding** 4. Unpublished conference paper 5. Magazine article 6. Unpublished

Structural Design Considerations and Challenges for Busan's Haeundae Resort Complex

釜山海云台度假区结构设计的思考与挑战

Kwang Ryang Chung
President | 董事长

Dong Yang Structural Engineers
东洋构造安全技术

Seoul, South Korea
首尔，韩国

Kwang Ryang Chung has experience in the structural design and analysis of many major commercial and residential projects, Based in Seoul, Dr. Chung has been the President of DONGYANG Structural Engineers Co., Ltd. since 1995. Prior to coming to DONGYANG, Chul ho Park has experience in the structural design and analysis for tall building and oversea project in DONGYANG.

Kwang Ryang Chung为很多大型商业和住宅项目做过结构设计和结构分析，经验丰富。他自1995年以来一直担任位于首尔的东洋结构工程有限公司的董事长。在加入东洋结构工程有限公司前，Chul ho Park就为东洋的高层建筑和海外项目做过结构设计和结构分析，有很丰富的从业经验。

Abstract | 摘要

In the early twentieth century, many countries were obsessed with high-rise buildings taller than 100 stories, and Korea was swept up in the challenge to build high-rise buildings. However, the effects of the economic recession in the USA caused many countries to experience an economic crisis. It seemed for a time that no more high-rise buildings would be constructed, but the recession didn't cause Korea to lose passion (see, for example, Jam-sil Lotte Tower and Haeundae Resort Project). Unlike some mega-projects in other countries, Haeundae Resort is being constructed with concrete belt-walls and a concrete outrigger system rather than steel belt-trusses and outriggers. Considerations of the technical aspects of construction, structural analysis and nonlinear analysis are presented in this paper.

Keywords: Concrete Belt Wall, Fire Resistant of High- Strength Concrete, Ground Reinforcement, Performance Based Design, Supertall and Tall Building Construction

在20世纪早期，许多城市热衷于建造高于100层的高层建筑，韩国也卷入了这一建造高层建筑的挑战中。但是，美国的经济衰退影响导致许多城市遭遇了经济危机，一段时间内应该不会建造更多的高层建筑了，但是衰退没有让韩国失去热情（参见蚕室乐天大楼及海云台度假酒店项目等）。和其他国家的超大项目不同，海云台度假酒店是由混凝土环带墙及混凝土外伸臂桁架系统建造而成，而非钢筋环带桁架及外伸臂桁架。本文展示了施工技术部分、结构分析及非线性分析中的多方面考量要素。

关键词：Concrete Belt Wall、耐火高强度混凝土、地基加固、性能设计、超高层建筑、高层建筑

I. Introduction

Busan Haeundae Resort Project, which was designed by Samoo Architects & Engineers along with Skidmore, Owings & Merrill LLP, is comprised of the 101-story, 411-meter Landmark Tower and two 85-story residential towers, each rising to 326 meters. Landmark Tower's structural system, designed by Chunglim, is composed of three belt walls and outriggers to resist the lateral load. The 85-story residential towers, with structural systems designed by Dongyang Structural Engineers Co., Ltd., also have three belt walls and two outriggers with fin and buttress walls. These structural systems enhance the buildings' robustness to resist the high wind load in Busan, Korea (Figure 1).

Because of the buildings' waterfront location, various expected problems had to be taken into consideration. These challenges to building design and construction required the following strategies:

- Strategy for high-strength concrete placement
- Strategy for the fire resistance of high-strength concrete

Figure 1. Bird's-eye view of Haeundae Resort (Source: SAMOO)
图1. 海云台酒店鸟瞰图（来源：SAMOO）

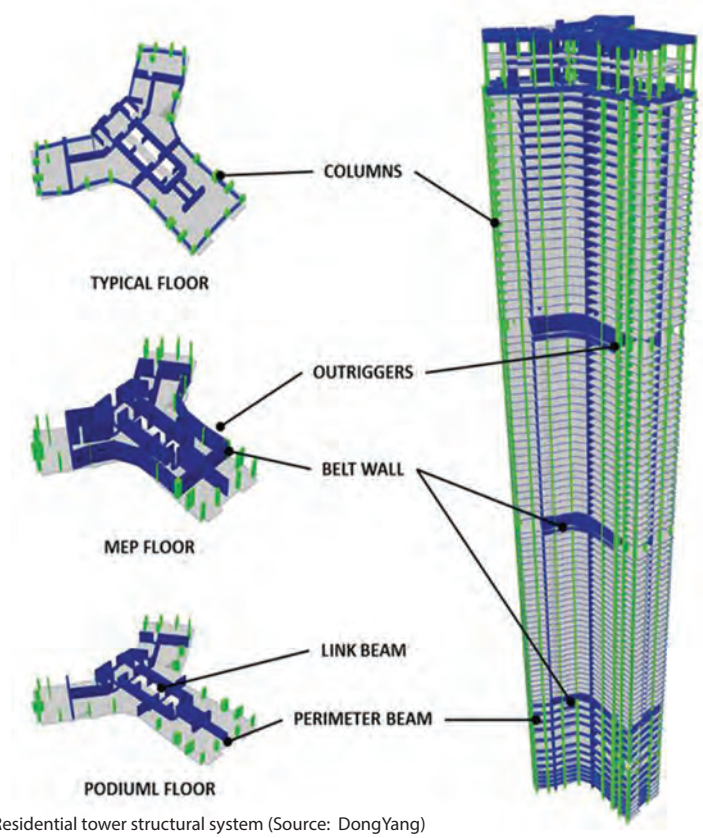

Figure 2. Residential tower structural system (Source: DongYang)
图2. 住宅楼结构系统（来源：DongYang）

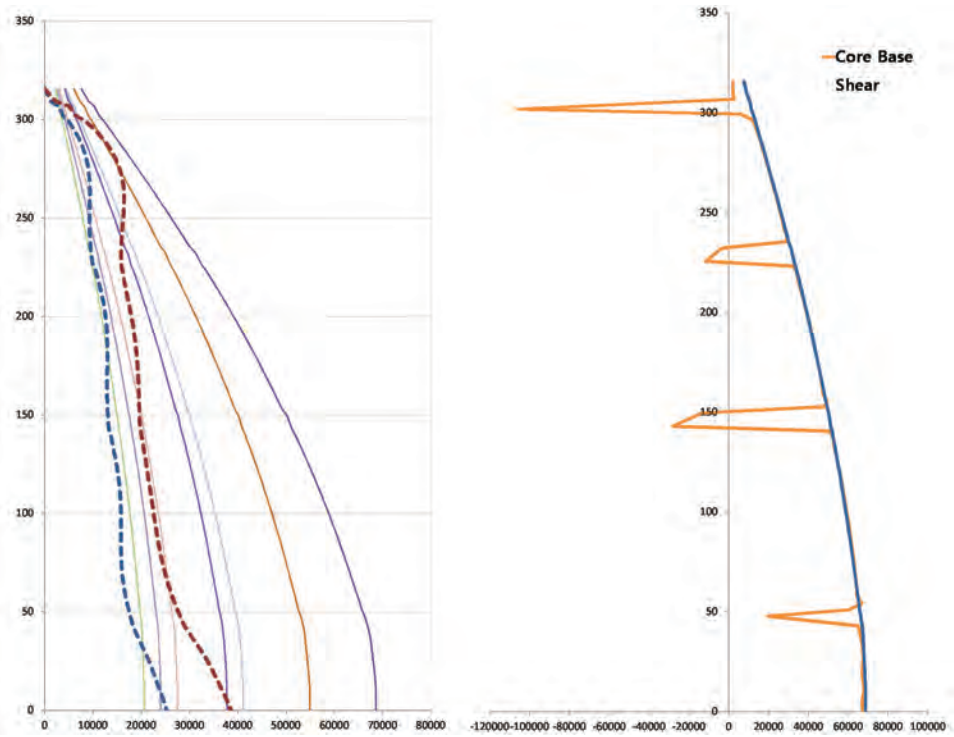

Figure 3. Base shear comparison (Source: DongYang)
图3. 底部剪力对比（来源：DongYang）

- Strategy for the ground reinforcement of the foundation
- Strategy for the seismic performance evaluation through nonlinear analysis

The four points mentioned above were the most important challenges of this project, as regards structural analysis and construction, each of which needed to be duly considered to carry out the project successfully (Figure 2 and 3).

II. Challenges

1. Construction Technology for High-Strength Concrete

"PosMent" was used on this project, a concrete material developed by POSCO Inc. PosMent, which uses slag generated by the steel manufacturing company, is an effective concrete for durability and strength because the slag can reduce concrete cracking due to the low heat of hydration. As the foundation

一、 介绍

釜山海云台度假区由Samoo建筑工程公司与Skidmore, Owings & Merrill LLP公司共同设计，由一座101层、高411米的地标楼和两座 85层、高326米的住宅楼组成。 由Chunglim公司设计的地标楼结构体系中包含三处用以抵御横向荷载的带状墙面和悬臂梁。而由Dongyang 结构工程有限公司设计的85层住宅大楼结构体系也含有三处带状墙面和两处带翼缘墙和前垛墙的伸臂。这些结构体系将增强建筑物的坚固性，抵抗韩国釜山的高风力荷载（图1）。

由于建筑傍水而建，我们需要将诸多可预见的问题纳入考虑范围。需采用以下策略应对建筑设计和施工中的挑战：

- 高强混凝土浇筑策略
- 高强混凝土抗火性能策略
- 地基加固策略
- 通过非线性分析进行抗震性能评估策略

就结构分析和建造方面，上述四点是本项目最大的挑战，应对每一项进行相应思考，以便本项目的成功开展（图2、3）。

二、 挑战

1. 高强度混凝土的建筑工艺

本项目使用由浦项制铁公司生产的PosMent混凝土。PosMent使用钢铁制造业公司产生的钢渣，是一种耐久性和强度都十分优秀的混凝土，原因在于钢渣可以减少由低水化热造成的混凝土裂缝。鉴于地标楼地基深度为 5.0 米，而住宅楼为 4.5 米，减少大体积混凝土的水化热十分必要。因此，通过使用PosMent 混凝土，成功实现了对大体积混凝土水化热的控制（图4）。

海云台度假区的地标楼和每幢住宅楼都有三层包含带状墙面的楼层。相对于钢质带状墙面，混凝土带状墙的刚度更高。然而，由于带状墙面受到混凝土浇筑和柱体收缩带来的附加应力，它的屈服强度可能被高估。因此需在刚度差异较大的翼缘墙和柱体间使用后浇连接，以将建筑所受的附加应力降至最低（图5）。

2. 高强混凝土耐火性能评估

由于高强混凝土易在高温下剥落，根据韩国建筑 规范(KBC2009) 要求，强度超过 50MPa的构件需进行剥落检验 。尤其当构件强度超过 60MPa时，必须采用实验方式进行检验，而强度介于50MPa至 60MPa 之间的构件则须用其它方法检验。此外，尽管高强混凝土柱体构件中混合了聚乙烯纤维，其内部芯梁使用的为60MPa 混凝土，因此需要通过实验和分

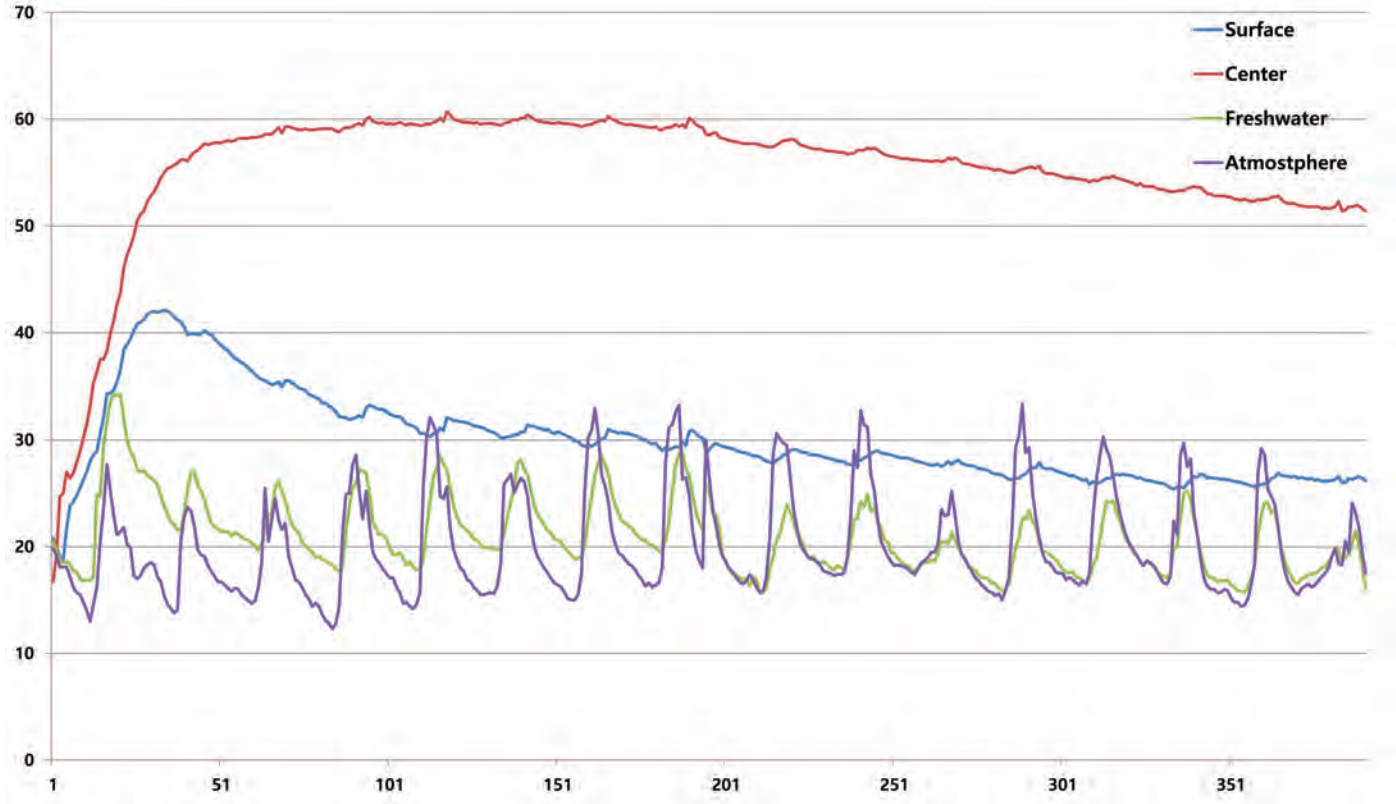

Figure 4. Mock-up test of hydration heat (Source: Posco)
图4. 水化热的模拟测试（来源：Posco）

depth of Landmark Tower is 5.0 meters and 4.5 meters for the residential towers, a reduction of hydration heat of the mass concrete was necessary. Therefore, hydration heat control of mass concrete was successfully achieved through the use of the PosMent material (Figure 4).

Landmark Tower and the residential towers of Haeundae Resort each have three belt-wall stories. Relative to steel belt-walls, concrete belt-walls have greater stiffness. However, it is possible to overestimate the yield strength of belt-walls because they receive additional stress while concrete is being placed and from column shortening. Therefore, delay joints will be installed in order to minimize the additional stress of the building, to be installed between fin walls and columns that have large differential stiffness (Figure 5).

2. Fire Resistance Performance Evaluation for High-Strength Concrete

Because of the tendency of high-strength concrete to experience spalling at high temperatures, Korean Building Code (KBC2009) requires that spalling be checked for members exceeding 50MPa strength. Especially, the strength of members which exceed 60MPa must be verified experimentally, and members that are between 50MPa and 60MPa must be checked by another method. Additionally, despite the fact that high-strength concrete column members are mixed with poly-fiber, inner core beams which use 60MPa concrete need to be checked for spalling caused by high temperature through experiment and analysis. The maximum strength used for core walls and columns is 80MPa concrete. KBC2009 does not have a specific article about temperature analysis. Therefore, in the case of some inner core beams with high-strength concrete, spalling was evaluated by applying ACI 216.1-07 and Eurocode for high-strength concrete exposed to a 3-hour fire.

SAFIR, a program for analyzing heat transfer, was used for temperature analysis of the structure. Mesh size was varied from 6mm to 20mm to increase the accuracy of FEM analysis, and the results indicated that there was an error of less than 1%. Therefore, the structure was analyzed with a 20mm mesh. Temperature

析来检验高温剥落。芯筒墙体和柱体应用的混凝土最高强度为80MPa。KBC2009并无有关温度分析的具体条款。因此，在评估高强混凝土内部芯梁的剥落时，采用了 ACI 216.1 07 和欧洲规范，即将高强混凝土在火中暴露 3 小时。

SAFIR是一个用于结构温度分析的热传递分析程序。为提高FEM（有限元建模）分析精度，网目尺寸6mm to 20mm不等，结果显示误差率小于1%。因此使用20mm网目对结构进行分析。考虑到EN-1992-1-2规定的数值，将温度条件设为构件表面500 ℃ 热负荷。

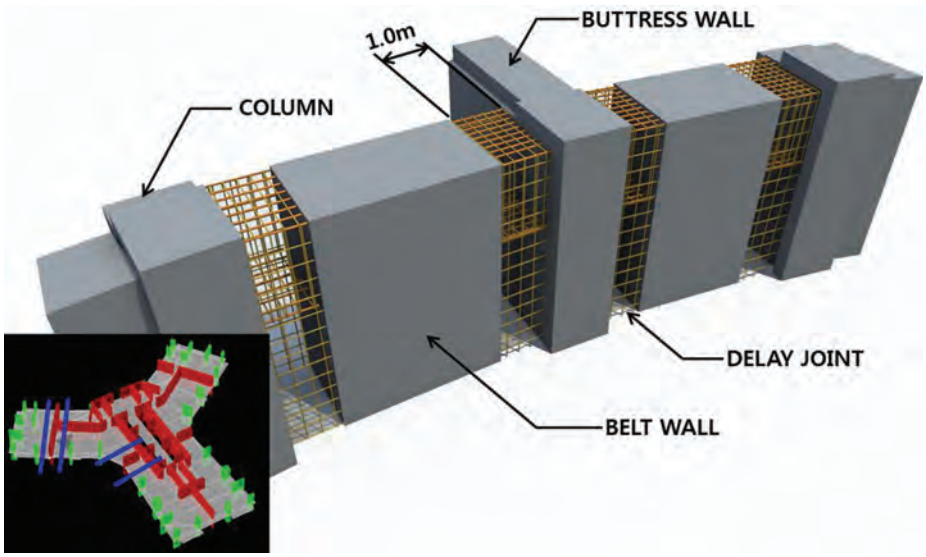

Figure 5. Delay joint of the tower belt-wall (Source: DongYang)
图5. 大楼环带墙后浇带（来源：DongYang）

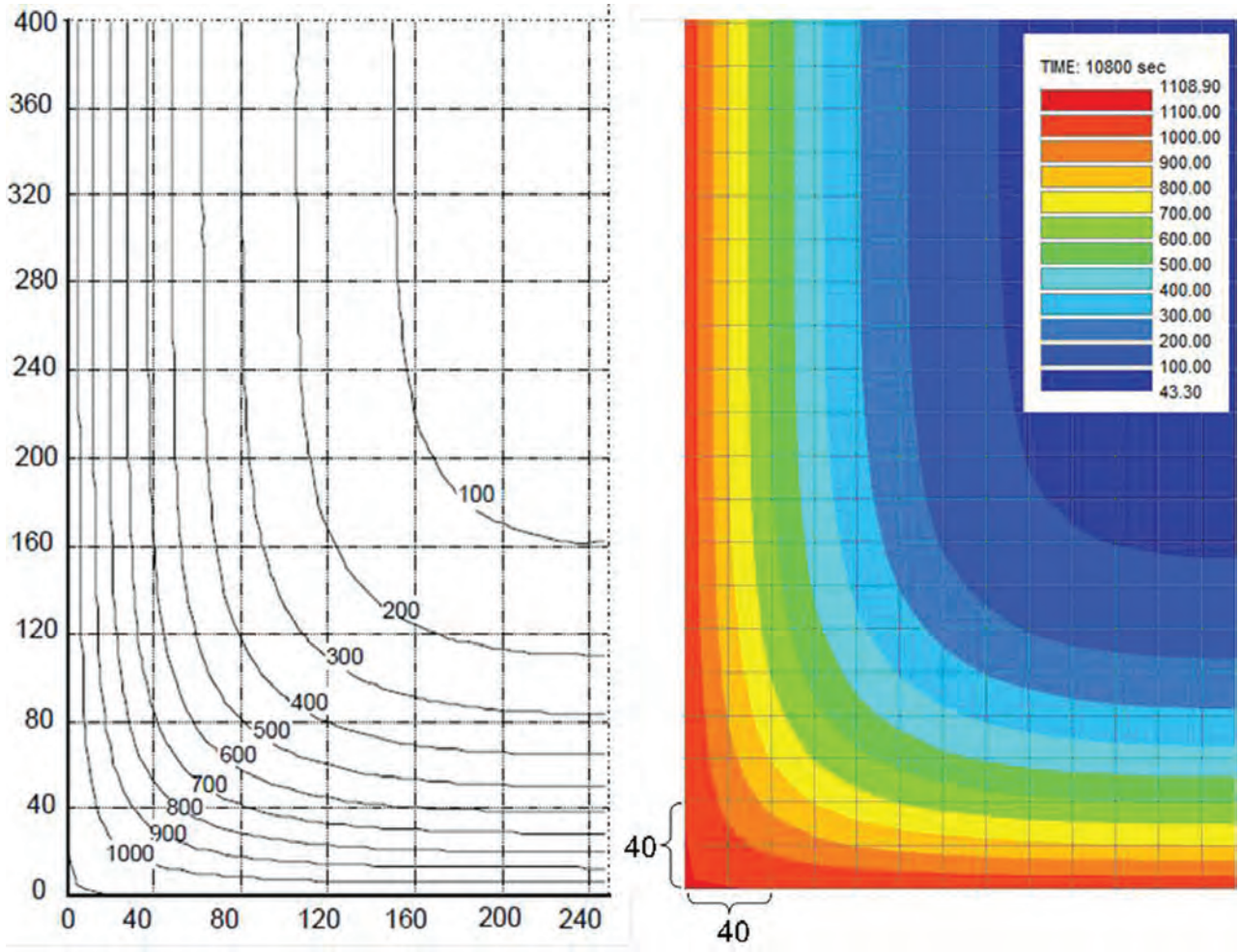

Figure 8. Comparison of temperature distributions of (Source: DongYang)
图8. 梁（500x800 mm）截面温度分布对比（来源：DongYang）

hours of exposure (R180) for a 500X800 mm beam, which is similar to the beam in this evaluation. Figure 8 represents the temperature distribution of a beam section derived from the heat transfer analysis of SAFIR for the same section size and heat condition as Figure 8 (units are ℃ and mm). According to the results of the comparison of the two cases, temperature distributions of beam sections are similar throughout, and isothermal line position and spacing are close in each case. Therefore, the heat transfer finite element analysis method used in this evaluation can predict the inner beam temperature distribution with great accuracy in case of a fire.

Temperature analysis for 500℃ fire resistance at LMT ground floor showed the reduction ratio of the concrete section to be between 48% and 83%. Therefore, it can be inferred that beam size has a correlation with fire resistance capacity. At PBB13A (300x450 mm), which has a relatively small section size, the reduction ratio of each concrete section and rebar is 53% and 59%. This means there is a large degree of reduction in material strength. By contrast, at the belt beam, which has a large section size, each reduction ratio of concrete and rebar is 85% and 92%, and this means the reduction degree of material strength is small.

The structural safety of an inner beam of the LMT ground floor core was evaluated for fire. In the case of moment, the load-strength ratio was a maximum of 0.82 at CB1 (400X650 mm), and, for shear, the maximum was 0.87 at CB22 (400X700 mm). Therefore, structural fire resistance capacity for the entire beam member showed no major problem.

III. Foundation Strategy

Despite the fact that this project is constructed above bedrock, some areas needed to be reinforced according to the results of excavation because parts of the ground did not have adequate strength to support a high-rise building. While the soil of both Landmark Tower and the two residential towers was replaced by mass concrete, some sections for Tower B had to be further reinforced by installing a disconnected pile on account of the depth of the replaced section. To evaluate the replacement and reinforcement of soil, analysis modeling progressed down to 100 meters below the foundation. The analysis reflected the bedrock level of drilling positions and drilling results. Also, RCD pile and replacement mass concrete was applied in the structural analysis. According to the results of analysis,

在公式中，T_f 为热源温度，测试使用标准的时间温度曲线。η_w 为热表面温度系数，而η_x（η_y）内部温度分布系数. 系数定义如下所示：

$$\eta_w = 1 - 0.0616 t_h^{-0.88}$$

$$\eta_x = 0.18 \ln(t_h / x^2) - 0.81$$

在公式中，t_h 为升温时间（单位：小时），而x为与热源的距离（单位：m）。使用单轴热流动公式预测距受热面不同距离（如27 mm、50 mm、82 mm）的温度随时间发生的变化。图6对结果进行了对比。

然而，Wickström 的公式针对的是160 mm宽的梁柱数据，如梁柱远宽于160mm，一般不建议使用。特别是由于预测位置热传递速度差异的存在，预测准确率将随距受热面距离增加而下降。为验证这一点，我们将SAFIR和Wickström公式预测的400 X 600 mm梁柱底部中央温度的结果显示在图6中。结果显示最高温度为354℃（SAFIR）和 316℃（Wickström），存在12%的温差率。产生此差异的推测原因为 Wickström 公式不能正确预测200mm距离侧面热源的影响。此外，此公式不能考虑三个受热面边

conditions were assumed as 500°C thermal load heated at member's surface, considering the values stipulated by EN-1992-1-2.

To examine the results of analysis, the results from SAFIR were compared with the temperature formula of Wickström (1986) and the temperature profile of Eurocode (EN 1992-1-2:2004). Wickström's temperature formula is derived from the Eurocode section related to heat transfer of a normal reinforced concrete member. This is a relatively simple method for estimating the temperature of a member, and it is used in various areas. Additional formulas are defined in two cases: Uniaxial Heat Flow, measuring one-dimensional heat transfer from one heat source, and Biaxial Flow, which measures two-dimensional plane heat transfer from two heat sources.

Uniaxial Heat Flow,

$$T_x = \eta_x \eta_w T_f$$

Biaxial Heat Flow,

$$T_{xy} = [\eta_w(\eta_x + \eta_y - 2\eta_x\eta_y) + \eta_x\eta_y]T_f$$

In these formulas, T_f is the temperature of the heat source, and a standard time-temperature curve was used in this examination. η_w is the coefficient of heat surface temperature and η_x (η_y) is the coefficient of inner distribution temperature. Definitions of these coefficients are shown below,

$$\eta_w = 1 - 0.0616 t_h^{-0.88}$$

$$\eta_x = 0.18 \ln(t_h / x^2) - 0.81$$

In these formulas, t_h is the heating time (unit: hours) and x is distance (unit: m) from the heating surface. Temperature change with time at various distances from the heating surface (i.e., 27 mm, 50 mm, 82 mm) is predicted by using the formula for Uniaxial Heat Flow. The results have been compared in Figure 6.

However, Wickström's formula is based on data for a 160 mm width beam, and it is generally not recommended in cases where beam width is far from 160 mm. Especially, as the distance from the heating surface increases, accuracy of predictions decrease due to heat transfer speed differences at the position of prediction. To verify this, the results of predicted temperatures from SAFIR and Wickström at the bottom center of 400X600 mm beams are shown in Figure 6. The results show that maximum temperatures were 354°C (SAFIR) and 316°C (Wickström), yielding a 12% temperature difference. The assumed reason for this is that Wickström's formula does not properly predict the effect of a side heat source

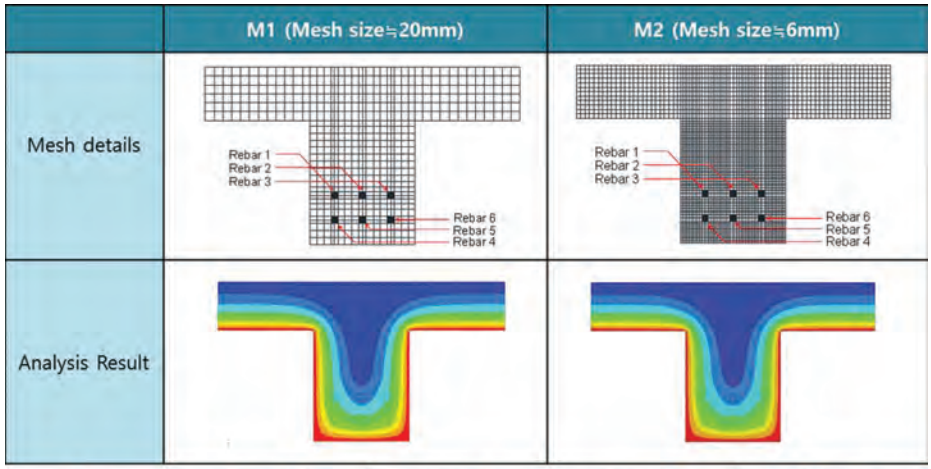

Rebar	Rebar 1, 3	Rebar 2	Rebar 4, 6	Rebar 5
M1	451.0 ℃	266.2 ℃	614.8 ℃	488.6 ℃
M2	451.7 ℃	265.4 ℃	615.0 ℃	485.4 ℃
error	0.16 %	0.30 %	0.03 %	0.65 %

Figure 6. Comparison of analysis results by mesh size (Source: DongYang)
图6. 网格尺寸分析结果对比（来源：DongYang）

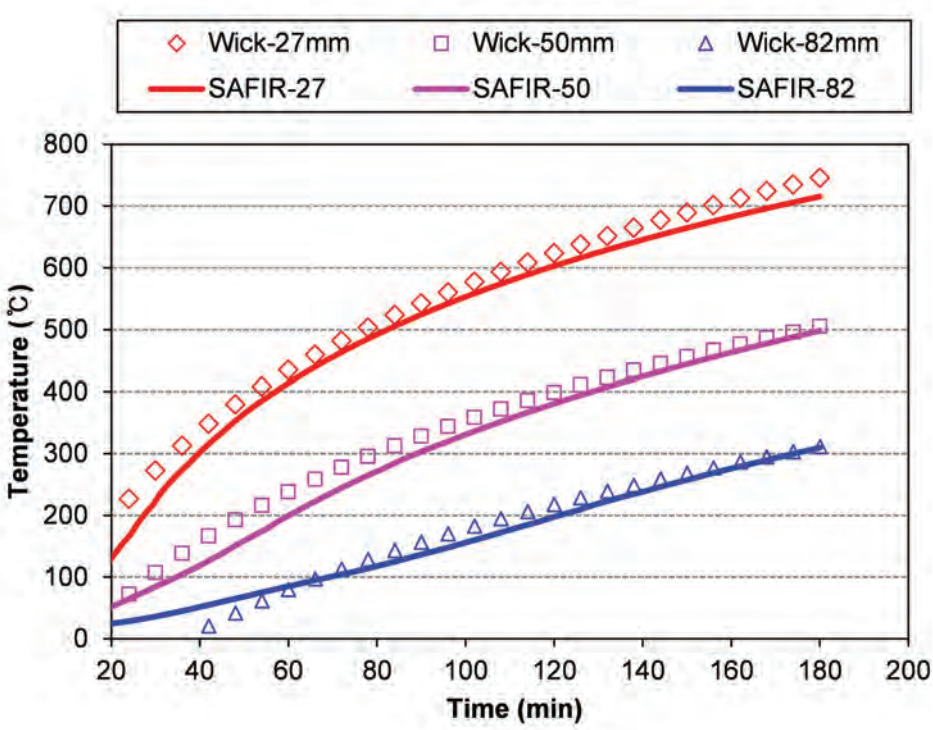

Figure 7. Comparison of close-range heat predictions (Source: DongYang)
图7. 近距离热力预测对比（来源：DongYang）

at 200 mm distance. Also, the formula is limited in that it cannot consider changes in heat characteristics which are derived from three

heating surface boundary conditions and the arrangement of main reinforcements. Therefore, to predict the inner temperature of a beam, it is considered appropriate to perform a heat transfer finite element analysis. The temperature profile is a diagram which displays the heat distribution of a heat-exposed beam section during a standard fire. It is included in Eurocode (EN 1992-1-2:2004) as part of fire resistant design and can be used as direct reference data when designing. Figure 7 is one temperature profile, and it represents the temperature distribution for 3

为了检查分析结果，需将SAFIR结果与Wickström （1986 年） 温度公式及欧洲规范（EN 1992-1-2:2004)的温度曲线进行对比。Wickström 温度公式源自欧洲规范中与普通钢筋混凝土构件热传递相关的部分，是一个相对简单的构件温度估算方法，应用于多个领域。另有两处使用了额外的公式：单轴热流动，用以测量从单一热源的单向热传递；及双轴热流动，测量源自两个热源的二维平面热传递。

单轴热流动

$$T_x = \eta_x \eta_w T_f$$

双轴热流动

$$T_{xy} = [\eta_w(\eta_x + \eta_y - 2\eta_x\eta_y) + \eta_x\eta_y]T_f$$

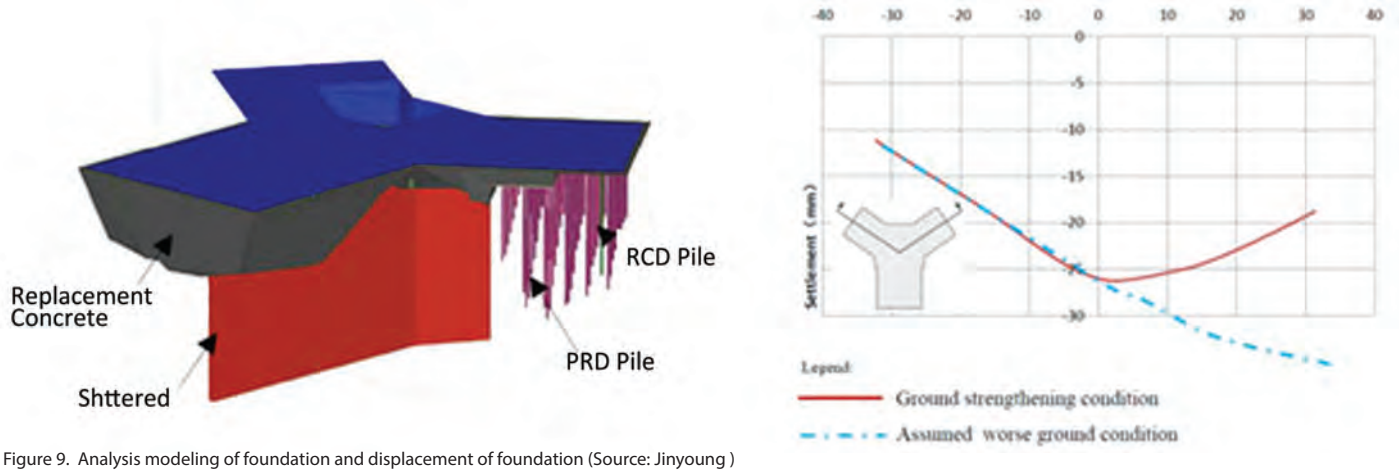

Figure 9. Analysis modeling of foundation and displacement of foundation (Source: Jinyoung)
图9. 基础建模分析与基础位移（来源：Jinyoung）

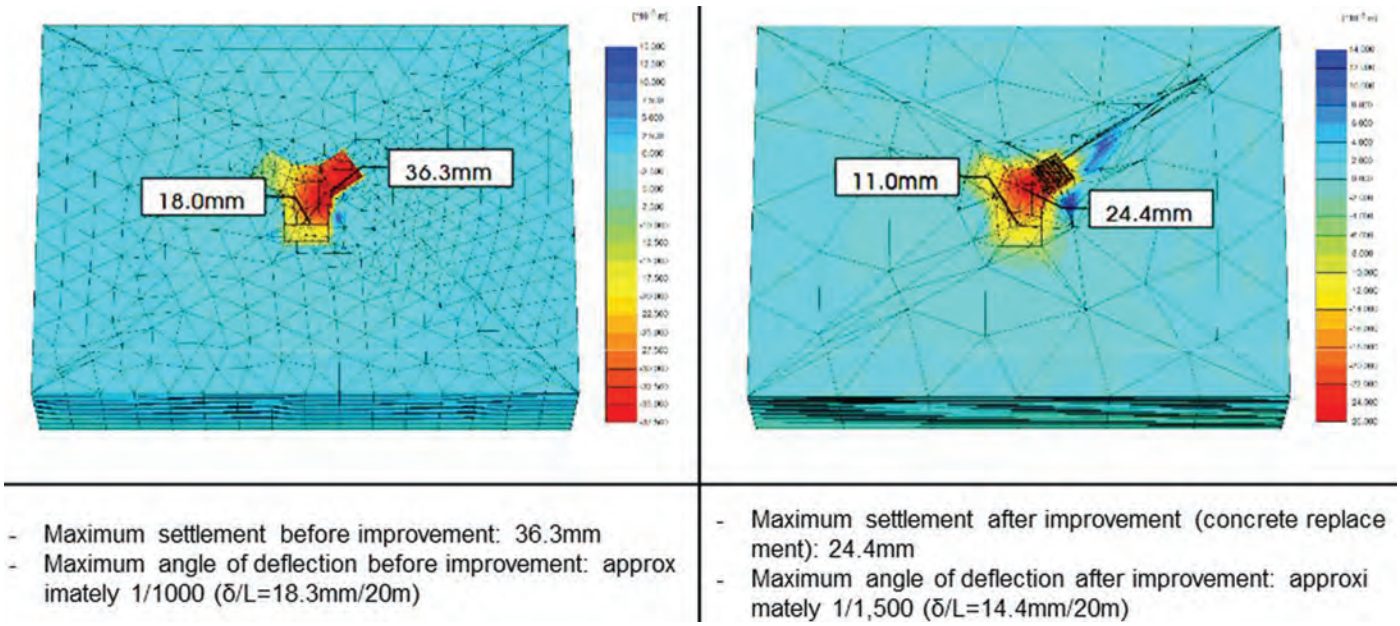

Figure 10. Comparative analysis of ground analytical models (Source: Jinyoung)
图10. 地基分析模型对比分析（来源：Jinyoung）

in the case of the residential towers, 29 mm was the maximum displacement to occur, and allowable soil bearing capacities of the residential towers and Landmark Tower were evaluated as 3,000 kN/m2 and 3,500 kN/m2. Especially in the case of Tower B, comparisons were made between before and after ground reinforcing, and Figure 9 compares displacements for whether a pile was installed or not. The results of ground settlement analysis showed the maximum settlement after ground improvement to be about 25 mm, and the maximum differential settlement is 1/1800, which is below the 1/500 limit and indicates safe behavior. Now that the ground bearing capacity tests for soil reinforcement have been completed, the towers are under construction in the foundation placement and above ground construction phases (Figure 10).

IV. Seismic Performance Review

As buildings and structures become higher and have more complicated shapes, traditional design methods based on a conservative lateral redundancy reduction coefficient design are limited for analyzing complicated structural systems. Therefore, a test was conducted to properly evaluate the seismic performance of the buildings. For the nonlinear time history analysis, the response spectrum was estimated by drawing a 5% damping response spectrum for each ground motion and applying the SRSS spectrum (square root of the sum of squares spectrum) for each building period. To evaluate building performance, a total of seven seismic wave cases were selected, and building performance objectives were evaluated at "special" seismic grade, which is actually one seismic grade higher than the designed seismic performance. Also, each structure was evaluated for lifesaving and immediate occupancy level.

The seven seismic wave cases below were applied for seismic performance evaluation of the building.

Each member's properties were similarly modeled by considering nonlinearity of

界和主钢筋影响下的温度特性变化，因此具有局限性。

因此，应进对梁柱内部温度的预测进行热传递有限元分析。温度曲线图显示在标准火灾情况下热暴露的梁柱截面热分布图。欧洲标准（EN 1992-1-2:2004)中此内容为防火设计的一部分，设计时可直接作参考数据使用。图7（a）为代表500 × 800 mm梁柱在3 个小时热暴露后（R180）的温度分布图。这一尺寸与本次评估中的梁柱宽度类似。图8代表源自SAFIR热传递分析的梁柱截面温度分布，该截面尺寸及热条件与图8（a）相同。（单位为 ℃ 和mm）。根据对两种情况进行比较的结果，截面温度分布自始自终一致，而两种情况中的等温线位置和间距均类似。因此，本次评估所用热传递有限元分析方法可十分精确地预测火灾中梁内温度的分布。

LMT地面楼层的500℃耐火温度分析显示混凝土截面的减速比在48%至83%之间。由此可推断梁柱尺寸与耐火性之间具有相关性。在截面尺寸相对较小的PBB13A（300 × 450mm），混凝土截面和钢筋

Seismic Grade 抗震等级	Performance Objectives 抗震性能目标	
	Performance Standards 抗震性能标准	Degree of Seismic Damage 地震破坏度
Special 特殊	Functional performance (or immediate occupancy) 1) 保证功能（或即时入住）1）	1.0 times of design spectrum acceleration 1倍设计谱加速度
	Life Safety 生命安全	1.5 times of design spectrum acceleration 1.5 倍设计谱加速度
I 一级	Life Safety 生命安全	1.2 times of design spectrum acceleration 1.2 倍设计谱加速度
II 二级	Life Safety 生命安全	1.0 times of design spectrum acceleration 1倍设计谱加速度

1. Decided by target performance standard of user and designer
1. 由用户或设计者所设的目标性能标准决定
2. According to 0306.3 Degrees of seismic damage in revised KBC2015
2. 根据KBC2015修订版第0306.3款地震破坏度

Figure 11. Seismic performance objectives (Source: DongYang)
图11. 抗震性能目标（来源：DongYang）

No. 项号.	Earthquake 地震	Year 年份	Station Name 站名	Magnitude 震级	Fault Type 断层类型	Rrup (km) 断层距(km)	Vs30 (m/sec) Vs30 参数 (m/sec)
1	Coalinga-01	1983	Slack Canyon	6.36	Reverse 逆断层	27.46	648.09
2	Coalinga-01	1983	Parkfield – Fault Zone 16	6.36	Reverse 逆断层	27.67	384.26
3	Parkfield-02_CA	2004	Hog Canyon	6	Strike Slip 走滑断层	5.28	376
4	Chi-Chi_Taiwan-03	1999	TCU116	6.2	Reverse 逆断层	22	493
5	Chi-Chi_Taiwan-06	1999	CHY028	6.3	Reverse 逆断层	34	543
6	San Fernando	1971	Lake Hughes #1	6.61	Reverse 逆断层	27.4	425.34
7	Mammoth Lakes-10	1983	Convict Creek	5.34	Strike Slip 走滑断层	6.5	382.12

Figure 12. Time history data for seismic performance evaluation (Source: DongYang)
图12. 抗震性能评估历史数据（来源：DongYang）

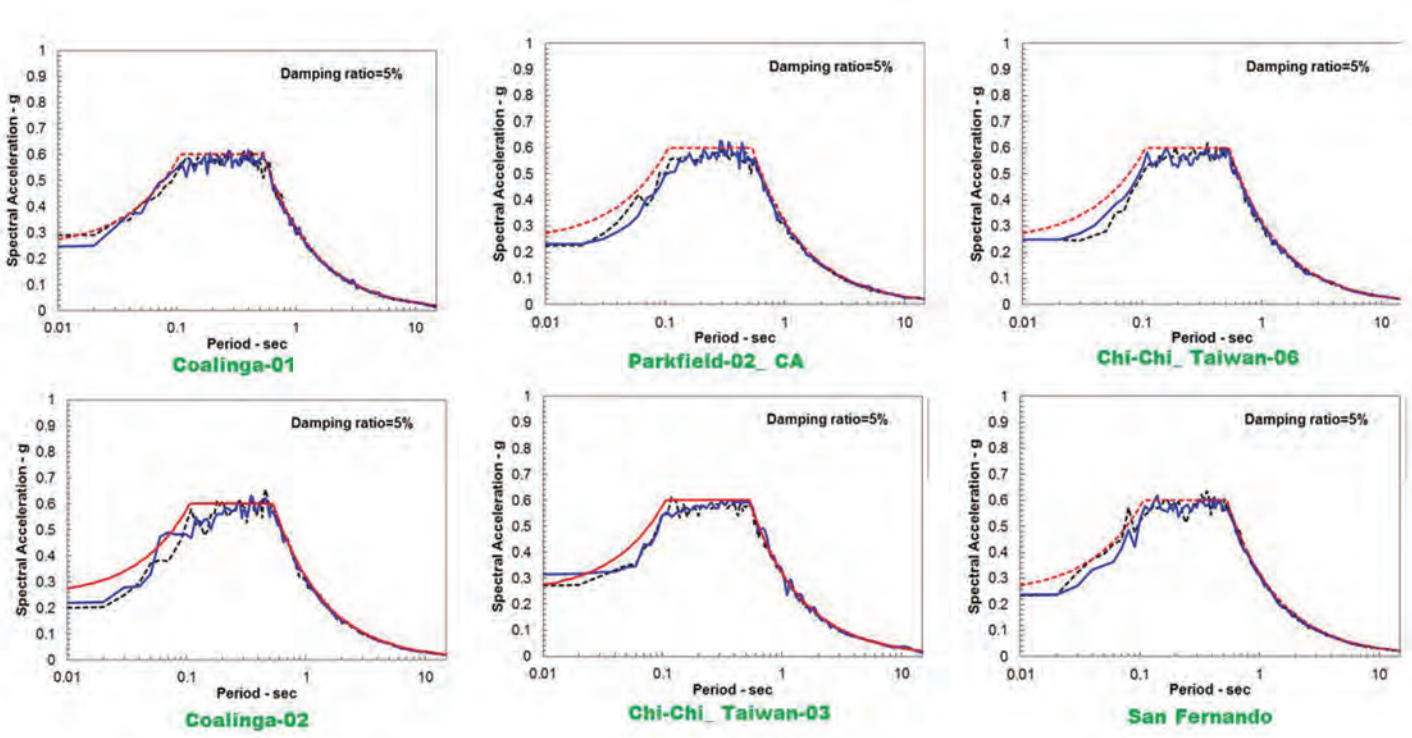

Figure 13. Time history data (Source: DongYang)
图13. 时程数据（来源：DongYang）

material, which is different from elastic analysis. Especially, fiber element and inelastic shear material are applied to the properties of core wall and belt wall.

The resort complex is located on the waterfront in the Haeundae District (in the city of Busan on Korea's southern coast) and is affected by a high wind load. The wind load in KBC2009, which is a factored load, has a return period of more than 6,000 years, and Busan is in an area which has the highest wind load in the country. Also, because of the characteristics of high-rise buildings, Landmark Tower and the residential towers have long-period properties of 9.13s and 7.46s. Therefore, the wind load effect which influences the building is about 2 to 2.5 times the effect of seismic load. The complex, however, was evaluated using nonlinear analysis software Perform 3D for the accurate performance evaluation of earthquakes. The model of the building includes nonlinear properties of materials, nonlinear force-deformation behavior of elements that are part of the seismic force resisting system, and acceptance criteria for deformations (plastic rotations, drifts, strains, etc.) based on ASCE 41-13. Seven pairs of time history data, recorded during reference earthquakes and adjusted for this project, were used (Figures 11, 12 and 13).

Although inelastic behavior in several elements was observed, acceptance criteria defined in ASCE 41-13 are satisfied. Therefore, lateral

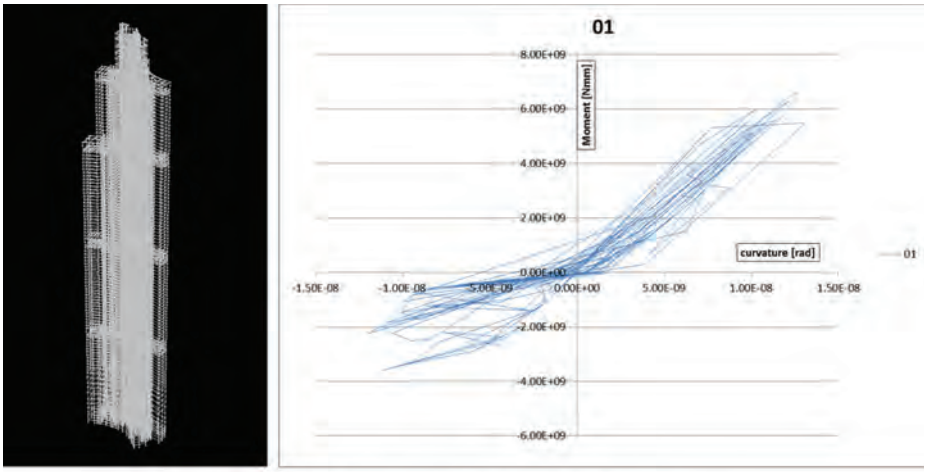

Figure 14. Nonlinear analysis model results for the belt-wall (Source: DongYang)
图14. 环带墙结果非线性分析模型（来源：DongYang）

elements have been studied for their own seismic capacity (Figure 14), as shown below:

1. Shear Walls

a. Plastic rotation of walls

- Plastic hinge rotation in all wall piers satisfies acceptance criteria for life safety specified in ASCE 41-13, Table 10-19. At the belt wall level, as well as two levels above and below it, some of the walls experience plastic hinge rotation between 0.3 and 0.5 of acceptable values. On other levels, plastic hinge rotation is below the limit value of 0.3.
- Two wall elements of the crown level (floor 85F PIT) experience plastic rotation higher than acceptable limits. However, those walls are not part of the seismic force resisting system and are supported on the transfer beam.

b. Total drift ratio

- Acceptance criteria for total drift of the wall are specified in ASCE 41-13, Table 10-20. The maximum usage ratio for wall drift in shear walls is below 0.5.

2. Coupling Beams

a. Plastic hinge rotation

- Plastic hinges were defined in both ends of coupling beams. Measured values of plastic hinge rotations did not exceed 0.3 of the limit value defined in Table 10-19 of ASCE 41-13.

b. Chord rotation

- Chord rotation of the coupling beam is connected with drift in shear walls. The limit values are defined in Table 10-20 of ASCE 41-13. Several beams in the model experienced chord drifts between 0.3 and 0.4 of the limit value.

3. Belt Walls

- Belt walls work like deep beams, so the source of nonlinearity is likely to be the horizontal axial-bending and/or in-plane shear. General wall element with fibers in two perpendiculars was used together with inelastic shear material.

Based on a preliminary analysis, the building is capable of resisting a strong earthquake across optimal life safety performance levels. Nonlinear behavior is observed in several elements, but acceptance criteria are not exceeded. The exception is two wall piers at the crown level, where damage due to plastic hinge rotation may happen. However, as those walls are not part of the seismic force resisting system and their role is purely to withstand gravity loads, the overall behavior of the building is not influenced by their failure. Design of those elements should be revised to provide higher values for flexural stiffness.

的减速比为53%和59%。这表明着材料强度有较大程度的减弱。与此相反，在带状墙面区域，由于截面尺寸大，混凝土截面和钢筋的减速比为85%和 92%，这表明材料强度的减损较小。我们对 LMT 地面楼层的核心内梁进行了火灾结构安全评估。目前情况下，最高负荷强度比在 CB1（400 X 650mm），数值为0.82，而在剪力墙，值是为0.87，出现在CB22（400 X 700 mm）。因此，梁构件整体的耐火性能并无大问题。

三、地基策略

尽管本项目建于基岩之上，由于部分地面的强度不足以支撑高层建筑，我们仍应根据挖掘结果对一些区域进=行加固。除用大体积混凝土对地标楼和两栋住宅楼基底的土壤进行置换外，还应根据置换区域深度的不同，在B楼的部分区域安装桩顶脱离筏板的桩柱进行进一步加固。我们开展了深达地基下100米的分析建模，用以评估土壤置换和加固的效果。分析反映了钻孔位置的基岩水平及钻探结果。此外，反循环钻孔成桩和大体积混凝土置换也应用在结构分析中。根据分析，对于住宅楼，发生的最大位移为29mm，而住宅楼和地标楼的容许土壤承载能力的评估为 3,000 kN/m2和 3,500 kN/m2。我们特别对B楼的地基加固前后情况进行了对比，图 9 比较了安置桩基与否的位移情况。地面沉降分析结果显示地面加固后最大沉降值约为 25 mm，最大不均匀沉降为 1/1800，低于 1/500 的限值，属安全状态。目前对土壤加固的地面承载能力测试已完成，建筑施工正处于地基浇筑和地面施工阶段。

五、抗震性能评估

随着建筑物和结构变得更高、出现更多复杂形状，基于保守性横向冗余减少系数的传统设计方法在对复杂结构体系进行分析时效果有限。因此，应进行测试以正确评估建筑物的抗震性能。在非线性时程分析中，通过为每个地面运动绘制 5%的阻尼响应谱，以及对每一个建设期应用 SRSS 谱 （振型组合方法谱），对响应谱进行估算。评估建筑抗震性时，共选取七个地震波，并将建筑的抗震性能目标设为”特殊”的抗震等级，这比设计抗震性能高一个等级。此外对每个结构进行了救生和即时入住水平的评估。

通过以下七个地震波例子评估建筑物的抗震性能。

与弹性分析不同，模拟每个构件的特性时均考虑到了材料的非线性。尤其在芯筒墙

V. Conclusion

Korean high-rise buildings have been designed with a variety of structural systems. In contrast to most high-rise buildings in Korea, which are made of steel, the Haeundae Resort Complex in Busan uses reinforced concrete. To solve the problems that can arise from the use of reinforced concrete, studies were carried out to improve workability and efficiency of the structure, using both conventional methods plus new methods. The complex is under construction and is expected to be completed in 2019.

体和带状墙面特性中都应用了纤维元素及无弹性剪切材料的情况下。

度假区坐落海云台区水边（位于韩国南部海岸的釜山市）受高风力荷载影响。韩国建筑 规范 KBC2009中的风力荷载为系数负载，重现周期超过 6000 年，而釜山所受的风力荷载全国最高。此外，由于高层建筑的特点，地标楼和住宅楼分别具有9.13s和7.46s的长周期特性。因此，风力荷载对建筑的影响效应约为地震荷载的 2 至 2.5 倍。然而我们运用非线性分析软件对度假区建筑进行了精确的3D抗震评估。建筑模型包括材料的非线性特性、抗震体系部分元素的非线性受力变形性状，以及美国土木工程师协会标准ASCE 41 13规定的变形验收标准（塑性铰转动、位移、拉力等 ）。我们选取七对参考地震期间记录的时程数据并加以调整后用于此项目测试（图11–13）。

在某些元素中观察到了非弹性行为，但均符合美国土木工程师协会标准ASCE 41–13规定的验收标准。因此我们对侧向元素自身的抗震能力进行了研究图14，情况如下：

1. **剪力墙**
   a. 墙体塑性铰转动
      - 在所有壁墩的塑性铰转动均满足美国土木工程师协会标准ASCE 41–13表10–19规定的生命安全级别验收标准。在带状墙面层以及其上下各两层的位置，有一些墙壁出现介于可接受值0.3和0.5之间的塑性铰转动。在其他层面上，塑性铰链旋转值均低于0.3的限值。
      - 顶层（地面起第85层）有两个壁墩的塑性铰转动高于可接受限值。然而，这些墙壁并非抗震系统的一部分，且有传输梁对其支撑。

   b. 总位移率
      - 美国土木工程师协会标准ASCE 41–13表10–20定义了墙体总位移率的验收标准。剪力墙的墙位移率最大使用率应低于0.5。

2. **连梁**
   a. 塑性铰转动
      - 连梁两端均定义塑性铰转动。根据美国土木工程师协会标准ASCE 41–13表10–19，塑性铰转动测量值不应超过0.3的极限值。

   b. 弦旋转
      - 连梁的弦旋转与剪力墙位移相关。美国土木工程师协会标准ASCE 41–13表10–20对此有定义。模型中的数根连梁存在极限值0.3–0.4之间的弦旋转。

3. **带状墙面**
   - 带状墙面的作用与深梁类似，因此其非线性可能源自水平轴向弯曲和/或平面剪切。含纤维的常规墙元素与非弹性剪切材料在两垂直线间同时使用。

根据初步分析，建设具备在生命安全级别抵御强地震的性能。在某些元素中观察到了非线性行为，但均未超过验收标准，只有顶层的两个壁墩例外：此处可能因塑性铰转动而受损。但那些墙壁并非抗震体系的一部分，而仅用于承载重力荷载，因此它们的缺陷不会影响建筑物的整体性能。应该对那些元素的设计进行修改，以提供更高的抗弯刚度。

六、结论

韩国的高层建筑设计包含多种结构系统。与韩国的大多数钢构造高层建筑不同，釜山海云台度假区建筑采用了钢筋混凝土。为解决采用该材料可能引起的问题，我们对此进行研究，同时使用传统和新型方法，提高结构的可行性和效能。该度假村正在建设过程中，预计于2019年完工。

References:

Choi, H.K. and Choi, C.S. (2015). **"Temperature Estimation Method of Hollow Slab at Elevated Temperature",** Journal of Korean Society of Hazard Mitigation.

Chung, K.R. and Sunu, W. I. (2015). **"Outrigger Systems for Tall buildings in Korea".** International Journal of High-Rise Buildings. Vol 4, No. 3.

Kim, D.H. and Chung, K.R. (2009). **"Evolution of Tall Buildign Structural System",** Architectural Institute of Korea. 53(8), PP. 18~23.

Powell, G.H. (2007). **"Detailed Example of a Tall Shear Wall Building".** Berkeley, California: Computers & Structures inc.

Yoo, J.H., Kim, W.J. and Hong, S.B. (2014). **" Field Application of Concrete Using PosMent",** Journal of Korea Concrete Institute.